HHS Public Access

Author manuscript

J Tissue Eng Regen Med. Author manuscript; available in PMC 2019 September 12.

Published in final edited form as:

J Tissue Eng Regen Med. 2019 August ; 13(8): 1418–1429. doi:10.1002/term.2883.

Optimization of Photocrosslinked Gelatin/Hyaluronic Acid Hybrid Scaffold for the repair of cartilage defect

Hang Lin[1,3,*], **Angela M. Beck**[1,2], **Kazunori Shimomura**[1], **Jihee Sohn**[1], **Madalyn R. Fritch**[1,2], **Yuhao Deng**[1], **Evan J. Kilroy**[1,2], **Ying Tang**[1], **Peter G. Alexander**[1], **Rocky S. Tuan**[1,2,3,*]

[1]Center for Cellular and Molecular Engineering, Department of Orthopaedic Surgery, University of Pittsburgh School of Medicine, Pittsburgh, Pennsylvania

[2]Department of Bioengineering, Swanson School of Engineering, University of Pittsburgh, Pittsburgh, Pennsylvania

[3]McGowan Institute of Regenerative Medicine, University of Pittsburgh, Pittsburgh, Pittsburgh, Pennsylvania

Summary

There is no therapy currently available for fully repair of articular cartilage lesion. Our laboratory has recently developed a visible light-activatable methacrylated gelatin (mGL) hydrogel with the potential for cartilage regeneration. In this study, we further optimized mGL scaffolds by supplementing methacrylated hyaluronic acid (mHA), which has been shown to stimulate chondrogenesis via activation of critical cellular signaling pathways. We hypothesized that the introduction of an optimal ratio of mHA would enhance the biological properties of mGL scaffolds and augment chondrogenesis of human bone marrow-derived mesenchymal stem cells (hBMSCs). To test this hypothesis, hybrid scaffolds consisting of mGL and mHA at different weight ratios were fabricated with hBMSCs encapsulated at 20×10^6 cells/mL and maintained in a chondrogenesis-promoting medium. The chondrogenenic differentiation of hBMSCs within different scaffolds was estimated after 8 weeks of culture. Our results showed that mGL/mHA at a 9:1 (%, w/v) ratio resulted in the lowest hBMSC hypertrophy and highest glycosaminoglycan production, with slightly increased volume of the entire construct. The applicability of this optimally designed mGL/mHA hybrid scaffold for cartilage repair was then examined *in vivo*. A full-thickness cylindrical osteochondral defect was surgically created in the rabbit femoral condyle and a 3-dimensional cell-biomaterial construct was fabricated by *in situ* photo-crosslinking to fully fill the lesion site. The results showed that implantation of the mGL/mHA (9:1) construct resulted

[*]Address correspondence to: **Hang Lin, Ph.D.**, Center for Cellular and Molecular Engineering, Department of Orthopaedic Surgery, University of Pittsburgh School of Medicine, 450 Technology Drive, Room 239, Pittsburgh, PA, 15219, USA, Phone: 4126245503, Fax: 4126245544, hal46@pitt.edu; **Rocky S. Tuan, Ph.D.**, Center for Cellular and Molecular Engineering, Department of Orthopaedic Surgery, University of Pittsburgh School of Medicine, 450 Technology Drive, Room 221, Pittsburgh, PA, 15219, USA, Phone: 4126482603, Fax: 4126245544, rst13@pitt.edu.

Contribution Statement

H.L. and R.S.T. designed the entire study and wrote the manuscript. H.L. also participated the collection of all results. A.M.B generated Figure 1, 2, 3 and S1. K.Z. performed the animal surgery and contributed to Figure 6A, B. J.S. and M.R.F. generated Figure 6D and S3. Y. D. and E.J.K. generated Figure 4 and 5. Y.T. and P.G.A. contributed to Figure S2 and 6C. P.G.A also assisted the animal surgery and housing, as well as study design.

Conflict of Interest Statement

The authors declare that there is no conflict of interest.

in both cartilage and subchondral bone regeneration after 12 weeks, supporting its use as a promising scaffold for repair and resurfacing of articular cartilage defects in the clinical setting.

Keywords

Mesenchymal Stem Cells; Photocrosslinking Hydrogel; Gelatin; Hyaluronic acid; Chondrogenesis; Cartilage regeneration

1. INTRODUCTION

Hyaline cartilage is the connective tissue found at the surface of articular joints that permits frictionless motion and absorbs/distributes loads (Tuli, Li, & Tuan, 2003). Because of aging, repetitive joint use, and other factors, cartilage deteriorates and flakes or forming tiny crevices, eventually leading to osteoarthritis (OA) (Mueller & Tuan, 2011). This chronic degenerative disease of articular joints is the most common joint disorder in the United States, affecting about 10% of American adults (Park, Mendy, & Vieira, 2018). It should be also noted that more than half of the affected adults are younger than 65 years of age (Deshpande et al., 2016), requiring long-term disease management. Several treatment methods have been clinically used to restore joint function, such as osteochondral transplantation and microfracture(Richter, Schenck, Wascher, & Treme, 2016). However, therapeutic options for cartilage repair are scarce and do not yield adequate results (Reddi, Becerra, & Andrades, 2011). For example, osteochondral transplantation is a highly invasive procedure requiring large incisions and donor grafts that are not always readily available (Sherman et al., 2014). Microfracture, a less invasive procedure that involves microfenstration into the subchondral bone, has been shown to reduce pain and increase mobility in short-term follow-up, but it has limited long-term success (Albright & Daoud, 2017). Total knee arthroplasty (TKA) represents an effective solution for end-stage OA because it can relieve pain, correct leg deformity, and help patients resume normal activities. However, TKA is an invasive surgery that replaces damaged biological joints with artificial prostheses. Infection, stiffness, and the limited lifespan of prostheses represent major risk factors for revision or repeat surgery (Judge et al., 2012; Kahn, Soheili, & Schwarzkopf, 2013).

More recent innovative treatment methods for OA, which have been studied in the field of regenerative medicine, involve the use of cells, scaffolds, and growth factors to biologically reproduce articular cartilage at the defect site. Regarding cells from different sources, human adult stem cells have drawn the most attention because of their demonstrated ability to differentiate into chondrocytes, as well as exhibit immunosuppressive and anti-inflammatory effects (Caplan, 2009; Kolf, Cho, & Tuan, 2007; Petrie Aronin & Tuan, 2010). By virtue of their additional advantages that include ease of isolation and plasticity, human bone marrow derived-mesenchymal stem cells (hBMSCs) have been considered a prime candidate cell type for cartilage tissue regeneration (Noth, Rackwitz, Steinert, & Tuan, 2010). With the supplementation of inductive molecules, such as transforming growth factor beta (TGF-β), hBMSCs are able to differentiate into a phenotype comparable to native chondrocytes and

result in *de novo* formation of new cartilage tissues (Choi, Choi, Park, Kim, & Min, 2010; Fan et al., 2010; Zuk et al., 2001).

Biomaterial scaffolds, another critical component of regenerative medicine-based therapy, have been used to provide a microenvironment conducive to cartilage regeneration, and serve as the carrier for cells and growth factors (Choi et al., 2010). For years, different types of materials have been developed and tested to accelerate cartilage regeneration, with or without cells. In particular, hydrogel scaffolds are the most commonly used scaffold since they have many properties in common with articular cartilage. For example, they are highly hydrated, provide compressive strength, and permit load transfer from the environment to chondrocytes, similar to native cartilage (Spiller, Maher, & Lowman, 2011). To date, different types of natural and synthetic hydrogels have been tested in animal studies and clinical trials, including alginate/agarose, collagen, polyelectrolyte (Lam et al., 2016), and polyethylene glycol. For example, Dai et al. used scaffold-free fibrin to induce the regeneration of full-thickness cartilage defects (Dai, Liu, Ma, Wang, & Gao, 2016). Silk fibroin (Ribeiro et al., 2018) or bioprinted polycaprolactone (Theodoridis et al., 2019) scaffolds have also been explored for cartilage repair. Unfortunately, no specific hydrogel material has accurately reproduced the tissue properties of cartilage. Therefore, further investigations are needed to optimize hydrogel materials and preparation methods.

Gelatin, a denatured form of collagen that has been widely used in the clinical setting, is recognized as an alternative for cartilage repair. Gelatin retains many of the native molecular epitopes for cell adhesion and signal transduction in collagen that are important for maintaining a chondrocyte phenotype (Yue et al., 2015). Previously, we used a low-toxicity initiator, lithium phenyl-2,4,6-trimethylbenzoylphosphinate, to photocrosslink methacrylated gelatin (mGL), via gelation by visible light illumination (Lin, Cheng, Alexander, Beck, & Tuan, 2014). The protocol allows direct cell encapsulation and is capable of rapid generation of cell-laden scaffolds with high cell viability, without the use of ultraviolet light or protective barriers. Scaffolds fabricated using this method are biodegradable, biocompatible, and resistant to swelling and contraction. The scaffolds also exhibit excellent in situ space-filling qualities in both air and aqueous solutions, without the use of protective barriers (Lin et al., 2014).

In this study, we further optimized mGL scaffolds by supplementing bioactive polymers, such as hyaluronic acid (HA). HA is widely distributed throughout connective, epithelial, and neural tissue, and is incompressible, highly hydrated, and an important component of the extracellular matrix (ECM) that contributes to cell proliferation and migration (Pre, Conti, & Sbarbati, 2016). HA also effectively interacts with cells via cell surface receptors (CD44) to enhance chondrogenesis (Bian et al., 2013). For example, the addition of HA (0.5%, w/v) to gelatin (9.5%, w/v) constructs resulted in more rounded cell morphologies and enhanced chondrocyte phenotype and reparative function as assessed by gene expression and immunofluorescence, and increased quantity and distribution of the newly synthesized ECM throughout the construct (Levett, Melchels, et al., 2014). In addition, the introduction of gelatin (1.7%, w/v) into HA (4%, w/v) caused a significantly greater amount of cartilage-specific ECM components from hBMSCs, as compared to 4% HA scaffolds with stronger promotion of collagen type II expression (Angele et al., 2009). To date, whether the

introduction of HA into photocrosslinked mGL is able to enhance hBMSC chondrogenesis and cartilage formation *in vivo* remains unknown. We hypothesized that at an optimal ratio, the addition of HA would enhance the structural and biological properties of mGL scaffolds and augment hBMSC chondrogenesis, thus promoting cartilage regeneration *in vivo*. To test this, hybrid scaffolds were fabricated, consisting of mGL and mHA at different weight ratios, and their capacity to support chondrogenesis of encapsulated hBMSCs examined *in vitro*. The *in vivo* applicability of this novel and optimal mGL/mHA hybrid scaffold for cell-based articular cartilage repair was examined using a rabbit model. A full-thickness cylindrical osteochondral defect was surgically created in the rabbit femoral condyle and a 3-dimensional (3D) cell-biomaterial construct was fabricated *in situ* to fill the lesion site. The efficacy of neo-cartilage to repair the lesion site was examined at 12 weeks after implantation.

2. MATERIALS AND METHODS

2.1 Preparation of photoinitiator LAP

All chemicals used in this study were purchased from Sigma-Aldrich (St. Louis, MO) unless stated otherwise. The visible light-activated initiator lithium phenyl-2,4,6-trimethylbenzoylphosphinate (LAP) was synthesized according to a protocol developed by Fairbanks et al.(Fairbanks, Schwartz, Bowman, & Anseth, 2009), by reacting 2,4,6-trimethylbenzoyl chloride with dimethyl phenylphosphonite and lithium bromide.

2.2 Preparation of methacrylated gelatin (mGL)

mGL was synthesized using a previously reported procedure(Lin et al., 2014; Nichol et al., 2010; Van den Bulcke et al., 2000). In summary, gelatin type B was added to ddH_2O. The mixture was placed in a shaker at 37°C until the gelatin was fully dissolved. Next, methacrylic anhydride (MA) was added to the solution. The mixture was then placed in a 37°C shaker for 24 hours, to ensure the components fully reacted. The mGL solution was dialyzed for 4 days against ddH_2O at room temperature using 3500 NMWCO dialysis cassette (Thermo Scientific, Waltham, MA). After lyophilization, the mGL was stored in a desiccator for future use.

2.3 Preparation of methacrylated hyaluronic acid (mHA)

mHA was prepared by reacting MA with sodium hyaluronate (research grade, MW 66-99 kDa, Lifecore, Chaska, MN),(Chung, Beecham, Mauck, & Burdick, 2009), using a procedure similar to that described above.

2.4 Fabrication of mGL/mHA hybrid hydrogel

mGL and mHA were dissolved in Hank's Balanced Salt Solution (HBSS) at 10%:0% (mGL:mHA,w/v), 9.5%:0.5%, 9%:1%, or 8.5%:1.5%, named as 10/0, 9.5/0.5, 9/1 and 8.5/1.5, respectively. The solution was adjusted to a pH of 7.4 using NaOH, and the photoinitiator LAP was then added to 0.15% w/v and stirred until fully dissolved. To form the hydrogel, monomer solution was poured into a silicon mold with 2mm height and 5mm diameter void space and covered with a glass coverslip. Then, one dental curing light (Mega Light CL, DBI America, Lutz, FL), producing light at 430nm-490nm and 1,400mW/cm^2

power, was applied to the top of the solution, as previously described.(Lin et al., 2014) After a total exposure time of 4 minutes, hybrid mGL/mHA hydrogels were cored out for immediate mechanical testing.

2.5 Mechanical testing of scaffolds with different mGL/mHA ratios

An electromechanical tester with 1000g load cell (ElectroForce 3200, Bose, Eden Prairie, MN) was used to test the mechanical properties of hydrogel scaffolds made with different mGL/mHA ratios, as previously described(Lin et al., 2014). Scaffold cylinders were placed between stainless steel discs, preloaded to 1g, and were subjected to 10% uniaxial and unconfined compression, using a constant rate (0.5%/s or 0.01mm/s). Compressive moduli of different scaffolds were determined from the slope of force versus displacement plots.

2.6 Human BMSCs(hBMSCs) isolation and expansion

With Institutional Review Board approval (University of Pittsburgh and University of Washington), hBMSCs were isolated from the bone marrow of femoral heads that were surgical waste from patients who underwent total hip arthroplasty. Freshly isolated cells were re-suspended in growth medium (GM, α-MEM containing 10% fetal bovine serum (FBS, Invitrogen, Carlsbad, CA), 1% Antibiotic-Antimycotic (Invitrogen), and 1 ng/ml FGF-2 (RayBiotech, Norcross, GA)), and then plated into 150 cm^2 tissue culture flasks (P0). Medium was changed every 3 to 4 days. Once 70 to 80% confluence was reached, cells were trypsinized (0.25% trypsin containing 1 mM EDTA, Invitrogen), one flask of which was split to 3 or 4 flasks (P1). Potential of hBMSCs was determined by their ability of osteogenic, adipogenic and chondrogenic differentiation upon appropriate stimulation (data not shown), which were characterized by the respective staining methods, alizarin red, safranin O, and oil red staining (Jiang et al., 2016). BMSCs pooled from 3 patients (54 years old female, 52 years old female and 57 years old male) were used in this study. All experiments were performed with passage 3 (P3) hBMSCs.

2.7 Encapsulation of hBMSCs into scaffolds for chondrogenesis

4 types of mGL/mHA monomer solution were prepared as described above. P3 hBMSCs pellets were re-suspend using monomer solution with a final density of 20×10^6/ml. The suspension was then poured into a mold (cylindrical void with 2mm height and 5mm diameter) and subjected to 4-minute visible light exposure, using a dental curing lamp. The cell-laden gelatin hydrogels were extracted and cultured in chondrogenesis-inducing medium (DMEM with high glucose (Gibco, 11995), 1% Antibiotic-Antimycotic, 0.1 μM dexamethasone, 50 μg/mL ascorbate 2-phosphate, 40 μg/mL L-proline (Sigma-Aldrich), 1×insulin-transferrin-selenium (ITS, Invitrogen), and 10ng/ml TGF-β3 (R&D Systems, Minneapolis, MN)).

Cell viability was assessed after 8 weeks of culture with a Live/Dead Viability/Cytotoxicity kit (Invitrogen) and observed by an epifluorescence microscopy (CKX 41, Olympus). Four fields (720μm×533μm for each) per sample were analyzed. Percentage of live cells was calculated based on the number of green stained cells divided by the total number of cells (green and red stained cells, dual stained counted once as dead). The total live cell number was further estimated using the CellTiter 96 AQueous Cell Proliferation Assay (Promega,

Madison, WI) after 8 weeks of culture. The dimension of constructs was also measured with a caliper.

2.8 Quantitative Real Time Polymerase Chain Reaction (Real-time PCR)

After 8 weeks, each construct was put into a 1.5ml Eppendorf tube with 600μl TRIZOL (Invitrogen) and crushed into tiny pieces, using a pestle. Total RNA was extracted using TRIZOL-chloroform method and purified by the RNeasyPlus mini kit (Qiagen, Hilden, Germany). The SuperScript IV kit (Invitrogen) was used to perform reverse transcription from mRNA to cDNA. Real-time PCR was conducted using the StepOnePlus thermocycler (Applied Biosystems, Foster City, CA) and SYBR Green Reaction Mix (Applied Biosystems). Sox9, Aggregan (AGG) and Collagen II (COL2) primer sequences are (Forward)AGCCTGCGCTCCAATGACT & (Reverse) TAATGGAACACGATGCCTTTCA, (Forward)GGCAATAGCAGGTTCACGTACA & (Reverse)CGATAACAGTCTTGCCCCACTT and (Forward)TTCCGCGACGTGGACAT & (Reverse)TCAAACTCGTTGACATCGAAGGT. Ribosomal protein L13a (RPL13A) was used as endogenous control, with forward primer sequence GACACAGGACCACTCATGAAGT and reverse sequence GTGCGGCTGCTTCCATAAG. Gene expression level was calculated using the Comparative CT (ΔΔCT) method.

2.9 Mechanical Testing of live cell-constructs

After 8 weeks culture in chondrogenic medium, the mechanical property of constructs was tested as described above. To calculate compressive moduli accurately, height and diameter of each construct were measured separately.

2.10 Sulfated glycosaminoglycan (GAG) quantitation

Total GAG deposited in scaffolds was quantitated to assess the production of cartilage matrix. After 28 days chondrogenic culture, each sample was digested overnight in papain solution (0.6ml/construct, 125 μg/ml in 0.1 M sodium acetate, 5 mM l-cysteine HCl, 0.05 M EDTA, and pH 6.0) at 60°C. After centrifugation at 13500×g for 5 minutes, proteoglycan content in supernatant was estimated by quantifying the amount of sulphated glycosaminoglycan (sGAG), using the dimethylmethylene blue dye binding assay (Blyscan, Biocolor, UK) with a chondroitin sulphate standard.

2.11 Histological analysis

For histology, constructs were fixed in 10% phosphate-buffered formalin (Fisher Chemical, Pittsburgh, PA), embedded in paraffin, sectioned at 8μm thickness, and stained with Safranin O/Fast green under standard protocols for sulfated proteoglycans and cell distribution analysis. Color images were captured using a microscope equipped with a digital camera (SZX 16 or CKX41, Olympus).

2.12 Animal study

All experimental procedures were approved by the Institutional Animal Care and Use Committee (IACUC) of the University of Pittsburgh (Protocol #: 13062028). New Zealand White rabbits (15-17 weeks. 3.7-3.9kg) were used in this study. Before shaving/prepping, an

anesthetic mixture, which consisted of ketamine 13mg/kg and xylazine 2.5mg/kg, was introduced intramuscularly to allow for the administration of isoflurane. Intubation and deep sleep was attained with isoflurane. A single perioperative dose of cephalothin sodium (20mg/kg) was administered intravenously. With the real-time monitoring of animal respiration and pulse, a medial parapatellar arthrotomy was performed, with a final incision 4cm in length to expose the medial femoral condyle. A 4 mm (diameter) drill bit was used to create a full thickness defect on femoral groove by removing the articular cartilage and subchondral bone to a depth of 3mm. The knee was irrigated during drilling, and the drill was operated at a slow rpm to prevent overheating. The wound was then gently irrigated with 0.9% neutral buffered saline for observation.

Monomer solution (mGL/mHA, 9:1, prepared as described above) was applied to the defect and photocrosslinked *in situ* to completely fill the lesion site with 4-minute visible light illumination. Defects without any treatment served as negative control group, named as “No treatment”. For the Sham group, animals underwent the same procedure except that osteochondral defects were not created. Afterwards, the muscle and skin were closed and the animals were monitored until ambulatory. An E-collar was used until the wounds were healed. Bilateral procedures were used (n=4 in sham group, and n=6 in other two groups).

The efficacy of the *in situ* formed neo-osteochondral tissue to repair the lesion site was estimated at 12 weeks post implantation. Animals were sacrificed with an overdose of sodium pentabarbitol. The defect area was exposed and imaged immediately for scoring. Afterwards, condyles were harvested and fixed in 10% formalin.

2.13 Micro-computed tomography analyses

Subchondral bone formation was estimated by micro-computed tomography (micro-CT, vivaCT 40, Scanco Medical, Switzerland). After obtaining two-dimensional image slices from the micro-CT, the view of interest (VOI) was uniformly delineated. 3D reconstructions were created using an appropriate threshold and kept constant throughout the analyses.

2.14 Statistical analysis

Each study was carried out with at least 3 experimental replicates (refer the actual number in Figure legends), and the results were expressed as the mean ± SD. Significant differences among the groups were determined by two-tailed Student’s t-test for two-group comparisons or ANOVA, followed by post-hoc analysis for multiple group comparisons. Significance was considered at $p < 0.05$(*) and $p < 0.01$(**).

3. RESULTS AND DISCUSSION

3.1 Scaffold mechanical properties

In native cartilage, there is more collagen than HA (13% vs 1% /wet weight) (Holmes, Bayliss, & Muir, 1988; Plumb & Aspden, 2005). Therefore, we used gelatin as the backbone and HA as the supplement in this study. Since high HA content (2%) was shown to result in significant scaffold swelling (Zawko, Suri, Truong, & Schmidt, 2009), which may cause adverse effects during tissue repair, such as tissue growth outside of the targeted defect, we

chose four gelatin/HA ratios at 10%/0%, 9.5%/0.5%, 9%/1%, 8.5%/1.5% (w/v), with HA composing no more than 2%, and designated these as groups 10/0, 9.5/0.5, 9/1, and 8.5/1.5.

To reduce variation due to HA leaching, a covalent bond should be established between HA and gelatin. Methacrylation is a common way to yield a double-bond conjugate to HA or gelatin, which initiates polymerization upon the attack of free radicals. As previously reported, we developed a visible light (VL)–activated crosslinking procedure to form hydrogel for cartilage tissue engineering (Lin et al., 2014). The mild photocrosslinking conditions of the procedure allow the incorporation of cells during the gelation process without compromising cell viability. In this study, we methacrylated HA (mHA) and gelatin (mGL) and thus formed mGL/mHA hybrid hydrogel scaffolds using the method we previously described (Lin et al., 2014).

As shown in Figure 1, right after being fabricated, without being cultured in aqueous solution, the compressive modulus of scaffolds increased as the HA ratio increased, which agreed with previously published articles (Levett, Hutmacher, Malda, & Klein, 2014). Such enhancement was expected, since our results and those from other labs showed that 3% mHA possesses similar mechanical properties to 10% mGL(Erickson, Kestle, Zellars, Dodge, et al., 2012). Therefore, mGL/mHA with an 8.5/1.5 ratio and the highest mHA amount, was significantly stronger than all other scaffolds (Figure 1).

3.2 *In vitro* chondrogenesis of MSCs within hydrogel

We then encapsulated hBMSCs into the mGL/mHA scaffolds with different ratios using a visible light-based photocrosslinking method established previously (Lin et al., 2014). Erickson et al. showed that encapsulating MSCs at a high density (60 million/mL) might produce higher sulfated glycosaminoglycan (GAG) than at low density (20 million/mL) for long-term culture, though this did not benefit the deposition of collagen for either short- or long-term culture (Erickson, Kestle, Zellars, Farrell, et al., 2012). Recently, we examined the effects of physiologically relevant cell densities (4, 8, 20, and 50×10^6 cells/mL) on chondrogenesis of hBMSCs incorporated in hydrogel constructs and determined that a cell seeding density of 20×10^6 cells/mL was most efficient in terms of extracellular matrix (ECM) production (on the basis of hydroxyproline and GAG content)(A. X. Sun et al., 2017). Therefore, a cell density of 20×10^6 cells/mL was chosen for this study. In addition, because culturing for a longer period (8 weeks) resulted in more GAG and collagen deposition to the constructs than short-term culture (2 or 4 weeks) (Erickson, Kestle, Zellars, Farrell, et al., 2012), we cultured cell-laden constructs in chondrogenic medium containing 10 ng/mL TGF-β3 up to 8 weeks for the final analysis.

Constructs supplemented with more HA showed a higher swelling ratio, characterized by increased height and diameter (Figure S1). Constructs in the 10/0 group maintained their original dimension without significant changes. This finding indicated that the mHA supplement may contribute significantly to the swelling of scaffolds, which had been demonstrated in another study using chitosan as the backbone (Correia et al., 2011). As reported previously, photocrosslinked HA underwent major swelling until reaching 1.5-4 times its original volume/weight, depending on the degree and concentration of methacrylation (Bencherif et al., 2008). Slight swelling is actually beneficial for future

clinical applications because it tightly fills the void space, which promotes graft fixation and tissue integration. However, overswelling could be problematic, causing issues such as tissue growth outside of the defect site. Currently, there is no established standard for optimal swelling ratio to achieve the best clinical outcome, requiring additional work in the future.

The short-term biocompatibility (day 1, 3, and 7) of visible light-based photocrosslinking was validated in our previous study (Lin et al., 2014). Here, we further analyzed the cell viability and cell number after longer-term (8 weeks) chondroinduction based on live/dead and MTS assays. Cells maintained high viability in all groups, as revealed by live/dead staining (Figure 2). The MTS assay showed that the addition of HA showed a trend towards a slight increase in total metabolic activities, suggesting the presence of more cells in hydrogel, though the difference was not statistically significant. In fact, cells inside hydrogel may have a hard time dividing , due to the physical barrier around them (Mohand-Kaci, Assoul, Martelly, Allaire, & Zidi, 2013). Because of its covalent bond, mGL degraded very slowly without the presence of exogenous collagenase or gelatinase, allowing no sufficient room for cell duplication (Lin et al., 2014; Zhao et al., 2016).

We then analyzed gene expression after 8 weeks of chondroinduction (Figure 3). It is surprising that the addition of HA led to a trend of decreased chondrogenic gene expression, including *SOX 9*, *COL2*, and *AGG*, although no significant differences were observed. In fact, a recent study also showed that supplementation with HA leads to a lower expression of collagen type II (Amann, Wolff, Breel, van Griensven, & Balmayor, 2017). These results disagreed with a another recent study, which indicated that higher HA resulted in a higher expression of chondrogenic gene marker genes at days 1, 4, and 7 (Pfeifer et al., 2016). However, it should be noted that such an enhancement was not observed after longer culture (21 days). Wu et al. investigated the gene expression up to 5 days after cell encapsulation and found HA inclusion significantly enhanced the expression of *SOX 9*, *COL2*, and *AGG* in fibrin, mainly through HA receptor CD44 (Wu et al., 2013). However, they did not report the results for longer culture times. In another study using fibrin/gelatin as the backbone, the supplementation of HA did enhance the expression of *COL2* and *AGG* after 21 days of chondroinduction (Sawatjui et al., 2015). However, the enhancement was not pronounced (<2 times). Overall, HA seems to benefit the initiation of chondrogenesis and such an effect is minor or slightly opposite after the establishment of chondrogenesis.

We also observed that HA (as low as 0.5%) reduced the expression of the hypertrophic marker gene, collagen type X (*COL10*). MSC hypertrophy is a recognized obstacle for MSC application in cartilage regeneration, which eventually causes cell ossification or apoptosis (M. M. Sun & Beier, 2014). To date, there have been no efficacious methods developed that can completely solve this problem. Our results suggested the potential of modulating scaffold composition to suppress hBMSC hypertrophy and enhance the quality of regenerated cartilage.

Although HA inclusion reduced the expression of chondrogenic gene expression based on the data at 8 weeks, we did observe higher deposition of GAG in the 9:1 and 8.5/1/5 groups (Figure 5A), which was not due to higher HA inclusion itself, since the method that we used to quantify sulfated GAG does not recognize HA. In fact, our results agreed with another

previous study, which showed that an increased inclusion of HA resulted in more GAG deposition in chitosan scaffolds (Correia et al., 2011). Such enhancement may have resulted from the beneficial effect of HA on chondrogenesis at the early stage, as discussed above, or the inhibition of HA on the release of newly synthesized GAG. The latter idea is supported by the Safranin O staining shown in Figure 4. In the 10/0 scaffold, GAG (indicated with red staining) did not distribute only around the cells. Instead, GAG was also observed in the area without cells, suggesting the movement of GAG within scaffolds. In addition, we observed a stain-free area in the margin of the constructs that decreased in size with the addition of HA. In the 9/1 and 8.5/1.5 constructs, we did not see such a GAG-free area. These results strongly suggest the capacity of HA to retain newly produced GAG. In native cartilage, HA serves as a 'backbone' for the array of aggrecan proteoglycans (McCarty, Russell, & Seed, 2000). Therefore, with the assistance of aggrecan and other proteoglycans generated from chondrogenic hBMSCs (Figure 3), HA in the scaffolds might bind the newly synthesized GAG in a similar manner as observed in native cartilage, thus enhancing the deposition of GAG.

We then tested the mechanical properties of constructs after 8 weeks of culture (Figure 5B). In general, the compressive modulus of constructs from all groups at 8 weeks was higher than those after 48 hours free swelling (Figure 5B), indicating the contribution of newly synthesized matrix on the mechanical property of the constructs. In addition, the compressive moduli reduced with increasing HA ratio in the constructs. As shown in Figure 5A, constructs from the 9/1 and 8.5/1/5 groups had higher GAG deposition. However, they also underwent a significantly higher swelling than other groups (Figure S1), which compromised their mechanical properties. In summary, compared with the other three groups, mGL/mHA at the 9:1 ratio was most effective at inhibiting hypertrophy, increasing GAG production, reducing the GAG-free area in the margin of the constructs, and increasing the mechanical properties with culture. Therefore, we determined the 9:1 ratio to be the optimal scaffold for MSC chondrogenesis. Its ability to repair cartilage defects was further tested in rabbit subjects.

3.3 Repair of cartilage defects in rabbit using optimal hydrogel

Different animal models have been used to test the reparative potential of tissue engineering products for cartilage repair, which close the gap between *in vitro* experiments and clinical application. Currently, the most recognized preclinical models include goats, sheep, and pigs, but they are cost-prohibitive and require adequate facilities (Chu, Szczodry, & Bruno, 2010). In our study, a rabbit model was employed because of the ease of handling and a reasonable joint size for surgery and scaffold implantation. Ideally, we would like to create a chondral defect to mimic full-thickness cartilage repair. However, such a defect is not feasible in rabbits because of the thin cartilage of the rabbit joint (300-500μm depth) (Rasanen & Messner, 1996). We thus generated a 4-mm diameter and 3-mm deep defect (Figure S2), which not only removed cartilage but also created a defect in the subchondral bone.

In this *in vivo* test, exogenous cells were not used, as they require an additional cell isolation culture process, or the usage of allograft cells, and these processes are not currently

compatible in clinical applications. Additionally, no evidence currently shows that naïve stem cell transplantation displays a superior reparative effect. For example, Guo et al. showed that the delivery of MSCs did not improve cartilage morphology for the repair of osteochondral defects in rabbits (Guo et al., 2010). In fact, increasing evidence shows that cells migrating from surrounding tissues may be sufficient for successful tissue regeneration (Kim et al., 2013; Solchaga et al., 2005). Therefore, in this study, we only applied mGL/mHA (9:1) to the defect site, without the usage of cells. As shown above, optimized mGL/mHA supports robust chondrogenesis, so we believe that mGL/mHA provides support for cell migration and promotes chondrogenesis and osteogenesis for both cartilage and bone (osteochondral) regeneration.

As shown in Figure S2, the mGL/mHA solution was applied to the defect site and subjected to 4 minutes of visible light illumination. The reason we performed the *in situ* fabrication was because tissue fixation and integration was enhanced by reducing the gap between the implant and surrounding tissues (24). After 12 weeks, animals were sacrificed, and the appearance of the defect area was imaged (Figure 6B). In the untreated group, the defect area was filled with newly regenerated tissues. However, the extensive cartilage loss was present over the entire joint surface. In comparison, defects treated with mGL/mHA were completely covered by a layer of white tissue, although it was slightly different from native cartilage in appearance. More importantly, we did not observe cartilage degeneration outside of the original surgical site, suggesting that mGL/mHA may prevent cartilage degeneration and the progression of osteoarthritis. Cartilage regeneration was then evaluated using a slight modification of the International Cartilage Repair Society (ICRS) scoring system, which is based on percentage defect filling, articular surface continuity, restoration of osteochondral architecture, repair tissue integration, cellular morphology of articular cartilage regeneration, and matrix staining (Willers, Chen, Wood, Xu, & Zheng, 2005). After applying mGL/mHA, the defects exhibited a significantly decreased score, suggesting an efficacious cartilage repair.

After the knees were fixed in formalin, bone formation was calculated via microCT. As shown in Figure 6C, the defect-only group without treatment showed limited new subchondral bone formation, and the edge of the defect was still clear and regular, preserving the mark of surgery. H&E staining in Figure S3 further showed the presence of scattered and minor bones in the defect site. However, in the group treated with mGL/mHA, robust bone formation was observed (Figures 6C & S3).

We then estimated cartilage formation by Safranin O staining. In the defect-only group, no GAG deposition was seen in the tissues filling the defect area, suggesting the presence of fibrous tissues (Figures 6D & S3). In the scaffold filling group, positive staining was observed, although the density and distribution was inferior to normal cartilage (Figure 6D). mGL and mHA are biodegradable biomaterials that were expected to degrade after transplantation, making space for cell migration onto or into the scaffolds. As shown in Figure 6D, we did observe a large number of cells within the defect site for all groups, suggesting exogenous cells may not be required for a successful regeneration. Limited cartilage tissue formation from mGL/mHA may be a result of insufficient chondroinductive signals. In this study, we did not introduce any chondroinductive growth factors such as

TGFβ within the scaffolds, as they are costly and affect other joint tissues (Blaney Davidson, van der Kraan, & van den Berg, 2007). For example, multiple injections of TGF-β induce synovial fibrosis and osteophytes in murine knee joints (van Beuningen, van der Kraan, Arntz, & van den Berg, 1994). To replace TGF-β, other growth factors have been examined. Kim et al. showed that insulin-like growth factor-1 (IGF-1) resulted in higher scores in subchondral bone morphology and increased amounts of chondrocyte and glycosaminoglycan in adjacent cartilage tissue when compared with a dual delivery of IGF-1 and TGF-β3, independent of the TGF-β3 release kinetics. The results suggest that the delivery of IGF-1 alone holds promise for osteochondral tissue engineering applications. In future studies, we may further test the application of mGL/mHA by supplementing IGF and/or other chondrosupportive growth factors.

CONCLUSION

In this study, mGL and mHA were mixed at different ratios and subjected to photocrosslinking to make hybrid hydrogel scaffolds. The compressive moduli of the constructs increased with the amount of HA. MSCs were able to undergo robust chondrogenesis and generate the best cartilage in mGL/mHA scaffolds at a ratio of 9:1, indicated by real time PCR, GAG assay, and mechanical testing. In addition, when implanted into the osteochondral defect in rabbits, mGL/mHA (9:1) scaffolds supported the generation of both cartilage and bone after 12 weeks, suggesting its potential in future clinical application for the repair of osteochondral defect.

Supplementary Material

Refer to Web version on PubMed Central for supplementary material.

ACKNOWLEDGEMENTS

The authors gratefully thank Dr. Paul Manner (University of Washington) for providing clinical tissue samples and Dr. Jian Tan (University of Pittsburgh) for isolating hBMSCs. We thank Peter Mittwede, MD, PhD, for editing a draft of this manuscript. This work was supported in part by the U.S. Department of Defense (W81XWH-10-1-0850, W81XWH-14-1-0217), the National Institutes of Health (1UG3TR002136 and 5R01EB019430) and the Pepper Grant (P30 AG024827).

REFERENCES

Albright JC, & Daoud AK (2017). Microfracture and Microfracture Plus. Clin Sports Med, 36(3), 501–507. Retrieved from https://www.ncbi.nlm.nih.gov/pubmed/28577709. doi:10.1016/j.csm.2017.02.012 [PubMed: 28577709]

Amann E, Wolff P, Breel E, van Griensven M, & Balmayor ER (2017). Hyaluronic acid facilitates chondrogenesis and matrix deposition of human adipose derived mesenchymal stem cells and human chondrocytes co-cultures. Acta Biomater, 52, 130–144. Retrieved from https://www.ncbi.nlm.nih.gov/pubmed/28131943. doi:10.1016/j.actbio.2017.01.064 [PubMed: 28131943]

Angele P, Muller R, Schumann D, Englert C, Zellner J, Johnstone B, … Kujat R (2009). Characterization of esterified hyaluronan-gelatin polymer composites suitable for chondrogenic differentiation of mesenchymal stem cells. J Biomed Mater Res A, 91(2), 416–427. Retrieved from https://www.ncbi.nlm.nih.gov/pubmed/18985778. doi:10.1002/jbm.a.32236 [PubMed: 18985778]

Bencherif SA, Srinivasan A, Horkay F, Hollinger JO, Matyjaszewski K, & Washburn NR (2008). Influence of the degree of methacrylation on hyaluronic acid hydrogels properties. Biomaterials,

29(12), 1739–1749. Retrieved from https://www.ncbi.nlm.nih.gov/pubmed/18234331. doi:10.1016/j.biomaterials.2007.11.047 [PubMed: 18234331]

Bian L, Hou C, Tous E, Rai R, Mauck RL, & Burdick JA (2013). The influence of hyaluronic acid hydrogel crosslinking density and macromolecular diffusivity on human MSC chondrogenesis and hypertrophy. Biomaterials, 34(2), 413–421. Retrieved from https://www.ncbi.nlm.nih.gov/pubmed/23084553. doi:10.1016/j.biomaterials.2012.09.052 [PubMed: 23084553]

Blaney Davidson EN, van der Kraan PM, & van den Berg WB (2007). TGF-beta and osteoarthritis. Osteoarthritis Cartilage, 15(6), 597–604. Retrieved from https://www.ncbi.nlm.nih.gov/pubmed/17391995. doi:10.1016/j.joca.2007.02.005 [PubMed: 17391995]

Caplan AI (2009). Why are MSCs therapeutic? New data: new insight. J Pathol, 217(2), 318–324. Retrieved from https://www.ncbi.nlm.nih.gov/pubmed/19023885. doi:10.1002/path.2469 [PubMed: 19023885]

Choi KH, Choi BH, Park SR, Kim BJ, & Min BH (2010). The chondrogenic differentiation of mesenchymal stem cells on an extracellular matrix scaffold derived from porcine chondrocytes. Biomaterials, 31(20), 5355–5365. Retrieved from https://www.ncbi.nlm.nih.gov/pubmed/20394983. doi:10.1016/j.biomaterials.2010.03.053 [PubMed: 20394983]

Chu CR, Szczodry M, & Bruno S (2010). Animal Models for Cartilage Regeneration and Repair. Tissue Engineering Part B-Reviews, 16(1), 105–115. Retrieved from <Go to ISI>://WOS:000274423200011. doi:10.1089/ten.teb.2009.0452 [PubMed: 19831641]

Chung C, Beecham M, Mauck RL, & Burdick JA (2009). The influence of degradation characteristics of hyaluronic acid hydrogels on in vitro neocartilage formation by mesenchymal stem cells. Biomaterials, 30(26), 4287–4296. Retrieved from https://www.ncbi.nlm.nih.gov/pubmed/19464053. doi:10.1016/j.biomaterials.2009.04.040 [PubMed: 19464053]

Correia CR, Moreira-Teixeira LS, Moroni L, Reis RL, van Blitterswijk CA, Karperien M, & Mano JF (2011). Chitosan Scaffolds Containing Hyaluronic Acid for Cartilage Tissue Engineering. Tissue Engineering Part C-Methods, 17(7), 717–730. Retrieved from <Go to ISI>://WOS:000292185800002. doi:10.1089/ten.tec.2010.0467 [PubMed: 21517692]

Dai YK, Liu G, Ma L, Wang DA, & Gao CY (2016). Cell-free macro-porous fibrin scaffolds for in situ inductive regeneration of full-thickness cartilage defects. Journal of Materials Chemistry B, 4(25), 4410–4419. Retrieved from <Go to ISI>://WOS:000378940600005. doi:10.1039/c6tb00681g

Deshpande BR, Katz JN, Solomon DH, Yelin EH, Hunter DJ, Messier SP, … Losina E (2016). Number of Persons With Symptomatic Knee Osteoarthritis in the US: Impact of Race and Ethnicity, Age, Sex, and Obesity. Arthritis Care Res (Hoboken), 68(12), 1743–1750. Retrieved from https://www.ncbi.nlm.nih.gov/pubmed/27014966. doi:10.1002/acr.22897 [PubMed: 27014966]

Erickson IE, Kestle SR, Zellars KH, Dodge GR, Burdick JA, & Mauck RL (2012). Improved cartilage repair via in vitro pre-maturation of MSC-seeded hyaluronic acid hydrogels. Biomed Mater, 7(2), 024110 Retrieved from https://www.ncbi.nlm.nih.gov/pubmed/22455999. doi:10.1088/1748-6041/7/2/024110 [PubMed: 22455999]

Erickson IE, Kestle SR, Zellars KH, Farrell MJ, Kim M, Burdick JA, & Mauck RL (2012). High mesenchymal stem cell seeding densities in hyaluronic acid hydrogels produce engineered cartilage with native tissue properties. Acta Biomater, 8(8), 3027–3034. Retrieved from https://www.ncbi.nlm.nih.gov/pubmed/22546516. doi:10.1016/j.actbio.2012.04.033 [PubMed: 22546516]

Fairbanks BD, Schwartz MP, Bowman CN, & Anseth KS (2009). Photoinitiated polymerization of PEG-diacrylate with lithium phenyl-2,4,6-trimethylbenzoylphosphinate: polymerization rate and cytocompatibility. Biomaterials, 30(35), 6702–6707. Retrieved from http://www.ncbi.nlm.nih.gov/pubmed/19783300. doi:10.1016/j.biomaterials.2009.08.055 [PubMed: 19783300]

Fan H, Tao H, Wu Y, Hu Y, Yan Y, & Luo Z (2010). TGF-beta3 immobilized PLGA-gelatin/chondroitin sulfate/hyaluronic acid hybrid scaffold for cartilage regeneration. J Biomed Mater Res A, 95(4), 982–992. Retrieved from https://www.ncbi.nlm.nih.gov/pubmed/20872747. doi:10.1002/jbm.a.32899 [PubMed: 20872747]

Guo X, Park H, Young S, Kretlow JD, van den Beucken JJ, Baggett LS, … Jansen JA (2010). Repair of osteochondral defects with biodegradable hydrogel composites encapsulating marrow mesenchymal stem cells in a rabbit model. Acta Biomater, 6(1), 39–47. Retrieved from https://www.ncbi.nlm.nih.gov/pubmed/19660580. doi:10.1016/j.actbio.2009.07.041 [PubMed: 19660580]

Holmes MW, Bayliss MT, & Muir H (1988). Hyaluronic acid in human articular cartilage. Age-related changes in content and size. Biochem J, 250(2), 435–441. Retrieved from https://www.ncbi.nlm.nih.gov/pubmed/3355532. [PubMed: 3355532]

Jiang Y, Cai Y, Zhang W, Yin Z, Hu C, Tong T, … Ouyang HW (2016). Human Cartilage-Derived Progenitor Cells From Committed Chondrocytes for Efficient Cartilage Repair and Regeneration. Stem Cells Transl Med, 5(6), 733–744. Retrieved from https://www.ncbi.nlm.nih.gov/pubmed/27130221. doi:10.5966/sctm.2015-0192 [PubMed: 27130221]

Judge A, Arden NK, Cooper C, Kassim Javaid M, Carr AJ, Field RE, & Dieppe PA (2012). Predictors of outcomes of total knee replacement surgery. Rheumatology (Oxford), 51(10), 1804–1813. Retrieved from https://www.ncbi.nlm.nih.gov/pubmed/22532699. doi:10.1093/rheumatology/kes075 [PubMed: 22532699]

Kahn TL, Soheili A, & Schwarzkopf R (2013). Outcomes of total knee arthroplasty in relation to preoperative patient-reported and radiographic measures: data from the osteoarthritis initiative. Geriatr Orthop Surg Rehabil, 4(4), 117–126. Retrieved from https://www.ncbi.nlm.nih.gov/pubmed/24600532. doi:10.1177/2151458514520634 [PubMed: 24600532]

Kim K, Lam J, Lu S, Spicer PP, Lueckgen A, Tabata Y, … Kasper FK (2013). Osteochondral tissue regeneration using a bilayered composite hydrogel with modulating dual growth factor release kinetics in a rabbit model. Journal of Controlled Release, 168(2), 166–178. Retrieved from <Go to ISI>://WOS:000319499200007. doi:10.1016/j.jconrel.2013.03.013 [PubMed: 23541928]

Kolf CM, Cho E, & Tuan RS (2007). Mesenchymal stromal cells. Biology of adult mesenchymal stem cells: regulation of niche, self-renewal and differentiation. Arthritis Res Ther, 9(1), 204 Retrieved from https://www.ncbi.nlm.nih.gov/pubmed/17316462. doi:10.1186/ar2116 [PubMed: 17316462]

Lam J, Clark EC, Fong EL, Lee EJ, Lu S, Tabata Y, & Mikos AG (2016). Evaluation of cell-laden polyelectrolyte hydrogels incorporating poly(L-Lysine) for applications in cartilage tissue engineering. Biomaterials, 83, 332–346. Retrieved from https://www.ncbi.nlm.nih.gov/pubmed/26799859. doi:10.1016/j.biomaterials.2016.01.020 [PubMed: 26799859]

Levett PA, Hutmacher DW, Malda J, & Klein TJ (2014). Hyaluronic acid enhances the mechanical properties of tissue-engineered cartilage constructs. PLoS One, 9(12), e113216 Retrieved from https://www.ncbi.nlm.nih.gov/pubmed/25438040. doi:10.1371/journal.pone.0113216 [PubMed: 25438040]

Levett PA, Melchels FP, Schrobback K, Hutmacher DW, Malda J, & Klein TJ (2014). A biomimetic extracellular matrix for cartilage tissue engineering centered on photocurable gelatin, hyaluronic acid and chondroitin sulfate. Acta Biomater, 10(1), 214–223. Retrieved from https://www.ncbi.nlm.nih.gov/pubmed/24140603. doi:10.1016/j.actbio.2013.10.005 [PubMed: 24140603]

Lin H, Cheng AW, Alexander PG, Beck AM, & Tuan RS (2014). Cartilage tissue engineering application of injectable gelatin hydrogel with in situ visible-light-activated gelation capability in both air and aqueous solution. Tissue Eng Part A, 20(17–18), 2402–2411. Retrieved from https://www.ncbi.nlm.nih.gov/pubmed/24575844. doi:10.1089/ten.TEA.2013.0642 [PubMed: 24575844]

McCarty MF, Russell AL, & Seed MP (2000). Sulfated glycosaminoglycans and glucosamine may synergize in promoting synovial hyaluronic acid synthesis. Medical Hypotheses, 54(5), 798–802. Retrieved from <Go to ISI>://WOS:000087487100026. doi:DOI 10.1054/mehy.1999.0954 [PubMed: 10859690]

Mohand-Kaci F, Assoul N, Martelly I, Allaire E, & Zidi M (2013). Optimized hyaluronic acid-hydrogel design and culture conditions for preservation of mesenchymal stem cell properties. Tissue Eng Part C Methods, 19(4), 288–298. Retrieved from https://www.ncbi.nlm.nih.gov/pubmed/22992013. doi:10.1089/ten.TEC.2012.0144 [PubMed: 22992013]

Mueller MB, & Tuan RS (2011). Anabolic/Catabolic balance in pathogenesis of osteoarthritis: identifying molecular targets. PM R, 3(6 Suppl 1), S3–11. Retrieved from https://www.ncbi.nlm.nih.gov/pubmed/21703577. doi:10.1016/j.pmrj.2011.05.009 [PubMed: 21703577]

Nichol JW, Koshy ST, Bae H, Hwang CM, Yamanlar S, & Khademhosseini A (2010). Cell-laden microengineered gelatin methacrylate hydrogels. Biomaterials, 31(21), 5536–5544. Retrieved from <Go to ISI>://000279092600006. doi:DOI 10.1016/j.biomaterials.2010.03.064 [PubMed: 20417964]

Noth U, Rackwitz L, Steinert AF, & Tuan RS (2010). Cell delivery therapeutics for musculoskeletal regeneration. Adv Drug Deliv Rev, 62(7–8), 765–783. Retrieved from https://www.ncbi.nlm.nih.gov/pubmed/20398712. doi:10.1016/j.addr.2010.04.004 [PubMed: 20398712]

Park J, Mendy A, & Vieira ER (2018). Various Types of Arthritis in the United States: Prevalence and Age-Related Trends From 1999 to 2014. American Journal of Public Health, 108(2), 256–258. Retrieved from <Go to ISI>://WOS:000439715700037. doi:10.2105/Ajph.2017.304179 [PubMed: 29267054]

Petrie Aronin CE, & Tuan RS (2010). Therapeutic potential of the immunomodulatory activities of adult mesenchymal stem cells. Birth Defects Res C Embryo Today, 90(1), 67–74. Retrieved from https://www.ncbi.nlm.nih.gov/pubmed/20301222. doi:10.1002/bdrc.20174 [PubMed: 20301222]

Pfeifer CG, Berner A, Koch M, Krutsch W, Kujat R, Angele P, … Zellner J (2016). Higher Ratios of Hyaluronic Acid Enhance Chondrogenic Differentiation of Human MSCs in a Hyaluronic Acid-Gelatin Composite Scaffold. Materials, 9(5). Retrieved from <Go to ISI>://WOS:000378628500076. doi:ARTN 38110.3390/ma9050381

Plumb MS, & Aspden RM (2005). The response of elderly human articular cartilage to mechanical stimuli in vitro. Osteoarthritis Cartilage, 13(12), 1084–1091. Retrieved from https://www.ncbi.nlm.nih.gov/pubmed/16154770. doi:10.1016/j.joca.2005.07.002 [PubMed: 16154770]

Pre ED, Conti G, & Sbarbati A (2016). Hyaluronic Acid (HA) Scaffolds and Multipotent Stromal Cells (MSCs) in Regenerative Medicine. Stem Cell Rev, 12(6), 664–681. Retrieved from https://www.ncbi.nlm.nih.gov/pubmed/27665291. doi:10.1007/s12015-016-9684-2

Rasanen T, & Messner K (1996). Regional variations of indentation stiffness and thickness of normal rabbit knee articular cartilage. J Biomed Mater Res, 31(4), 519–524. Retrieved from https://www.ncbi.nlm.nih.gov/pubmed/8836849. doi:10.1002/(SICI)1097-4636(199608)31:4<519::AID-JBM12>3.0.CO;2-B [PubMed: 8836849]

Reddi AH, Becerra J, & Andrades JA (2011). Nanomaterials and hydrogel scaffolds for articular cartilage regeneration. Tissue Eng Part B Rev, 17(5), 301–305. Retrieved from https://www.ncbi.nlm.nih.gov/pubmed/21595612. doi:10.1089/ten.TEB.2011.0141 [PubMed: 21595612]

Ribeiro VP, Morais AD, Maia FR, Canadas RF, Costa JB, Oliveira AL, … Reis RL (2018). Combinatory approach for developing silk fibroin scaffolds for cartilage regeneration. Acta Biomaterialia, 72, 167–181. Retrieved from <Go to ISI>://WOS:000432766900013. doi:10.1016/j.actbio.2018.03.047 [PubMed: 29626700]

Richter DL, Schenck RC Jr., Wascher DC, & Treme G (2016). Knee Articular Cartilage Repair and Restoration Techniques: A Review of the Literature. Sports Health, 8(2), 153–160. Retrieved from https://www.ncbi.nlm.nih.gov/pubmed/26502188. doi:10.1177/1941738115611350 [PubMed: 26502188]

Sawatjui N, Damrongrungruang T, Leeanansaksiri W, Jearanaikoon P, Hongeng S, & Limpaiboon T (2015). Silk fibroin/gelatin-chondroitin sulfate-hyaluronic acid effectively enhances in vitro chondrogenesis of bone marrow mesenchymal stem cells. Mater Sci Eng C Mater Biol Appl, 52, 90–96. Retrieved from https://www.ncbi.nlm.nih.gov/pubmed/25953544. doi:10.1016/j.msec.2015.03.043 [PubMed: 25953544]

Sherman SL, Garrity J, Bauer K, Cook J, Stannard J, & Bugbee W (2014). Fresh osteochondral allograft transplantation for the knee: current concepts. J Am Acad Orthop Surg, 22(2), 121–133. Retrieved from https://www.ncbi.nlm.nih.gov/pubmed/24486758. doi:10.5435/JAAOS-22-02-121 [PubMed: 24486758]

Solchaga LA, Temenoff JS, Gao J, Mikos AG, Caplan AI, & Goldberg VM (2005). Repair of osteochondral defects with hyaluronan- and polyester-based scaffolds. Osteoarthritis Cartilage, 13(4), 297–309. Retrieved from https://www.ncbi.nlm.nih.gov/pubmed/15780643. doi:10.1016/j.joca.2004.12.016 [PubMed: 15780643]

Spiller KL, Maher SA, & Lowman AM (2011). Hydrogels for the repair of articular cartilage defects. Tissue Eng Part B Rev, 17(4), 281–299. Retrieved from https://www.ncbi.nlm.nih.gov/pubmed/21510824. doi:10.1089/ten.TEB.2011.0077 [PubMed: 21510824]

Sun AX, Lin H, Fritch MR, Shen H, Alexander PG, DeHart M, & Tuan RS (2017). Chondrogenesis of human bone marrow mesenchymal stem cells in 3-dimensional, photocrosslinked hydrogel constructs: Effect of cell seeding density and material stiffness. Acta Biomater, 58, 302–311.

Retrieved from https://www.ncbi.nlm.nih.gov/pubmed/28611002. doi:10.1016/j.actbio.2017.06.016 [PubMed: 28611002]

Sun MM, & Beier F (2014). Chondrocyte hypertrophy in skeletal development, growth, and disease. Birth Defects Res C Embryo Today, 102(1), 74–82. Retrieved from https://www.ncbi.nlm.nih.gov/pubmed/24677724. doi:10.1002/bdrc.21062 [PubMed: 24677724]

Theodoridis K, Aggelidou E, Vavilis T, Manthou ME, Tsimponis A, Demiri EC, … Kritis A (2019). Hyaline cartilage next generation implants from adipose-tissue-derived mesenchymal stem cells: Comparative study on 3D-printed polycaprolactone scaffold patterns. J Tissue Eng Regen Med, 13(2), 342–355. Retrieved from https://www.ncbi.nlm.nih.gov/pubmed/30637991. doi:10.1002/term.2798 [PubMed: 30637991]

Tuli R, Li WJ, & Tuan RS (2003). Current state of cartilage tissue engineering. Arthritis Res Ther, 5(5), 235–238. Retrieved from https://www.ncbi.nlm.nih.gov/pubmed/12932283. doi:10.1186/ar991 [PubMed: 12932283]

van Beuningen HM, van der Kraan PM, Arntz OJ, & van den Berg WB (1994). Transforming growth factor-beta 1 stimulates articular chondrocyte proteoglycan synthesis and induces osteophyte formation in the murine knee joint. Lab Invest, 71(2), 279–290. Retrieved from https://www.ncbi.nlm.nih.gov/pubmed/8078307. [PubMed: 8078307]

Van den Bulcke AI, Bogdanov B, De Rooze N, Schacht EH, Cornelissen M, & Berghmans H (2000). Structural and rheological properties of methacrylamide modified gelatin hydrogels. Biomacromolecules, 1(1), 31–38. Retrieved from <Go to ISI>://000168746700006. doi:Doi 10.1021/Bm990017d [PubMed: 11709840]

Willers C, Chen J, Wood D, Xu J, & Zheng MH (2005). Autologous chondrocyte implantation with collagen bioscaffold for the treatment of osteochondral defects in rabbits. Tissue Eng, 11(7–8), 1065–1076. Retrieved from https://www.ncbi.nlm.nih.gov/pubmed/16144442. doi:10.1089/ten.2005.11.1065 [PubMed: 16144442]

Wu SC, Chen CH, Chang JK, Fu YC, Wang CK, Eswaramoorthy R, … Ho ML (2013). Hyaluronan initiates chondrogenesis mainly via CD44 in human adipose-derived stem cells. J Appl Physiol (1985), 114(11), 1610–1618. Retrieved from https://www.ncbi.nlm.nih.gov/pubmed/23449937. doi:10.1152/japplphysiol.01132.2012 [PubMed: 23449937]

Yue K, Trujillo-de Santiago G, Alvarez MM, Tamayol A, Annabi N, & Khademhosseini A (2015). Synthesis, properties, and biomedical applications of gelatin methacryloyl (GelMA) hydrogels. Biomaterials, 73, 254–271. Retrieved from https://www.ncbi.nlm.nih.gov/pubmed/26414409. doi:10.1016/j.biomaterials.2015.08.045 [PubMed: 26414409]

Zawko SA, Suri S, Truong Q, & Schmidt CE (2009). Photopatterned anisotropic swelling of dual-crosslinked hyaluronic acid hydrogels. Acta Biomater, 5(1), 14–22. Retrieved from https://www.ncbi.nlm.nih.gov/pubmed/18929518. doi:10.1016/j.actbio.2008.09.012 [PubMed: 18929518]

Zhao X, Lang Q, Yildirimer L, Lin ZY, Cui W, Annabi N, … Khademhosseini A (2016). Photocrosslinkable Gelatin Hydrogel for Epidermal Tissue Engineering. Adv Healthc Mater, 5(1), 108–118. Retrieved from https://www.ncbi.nlm.nih.gov/pubmed/25880725. doi:10.1002/adhm.201500005 [PubMed: 25880725]

Zuk PA, Zhu M, Mizuno H, Huang J, Futrell JW, Katz AJ, … Hedrick MH (2001). Multilineage cells from human adipose tissue: implications for cell-based therapies. Tissue Eng, 7(2), 211–228. Retrieved from https://www.ncbi.nlm.nih.gov/pubmed/11304456. doi:10.1089/107632701300062859 [PubMed: 11304456]

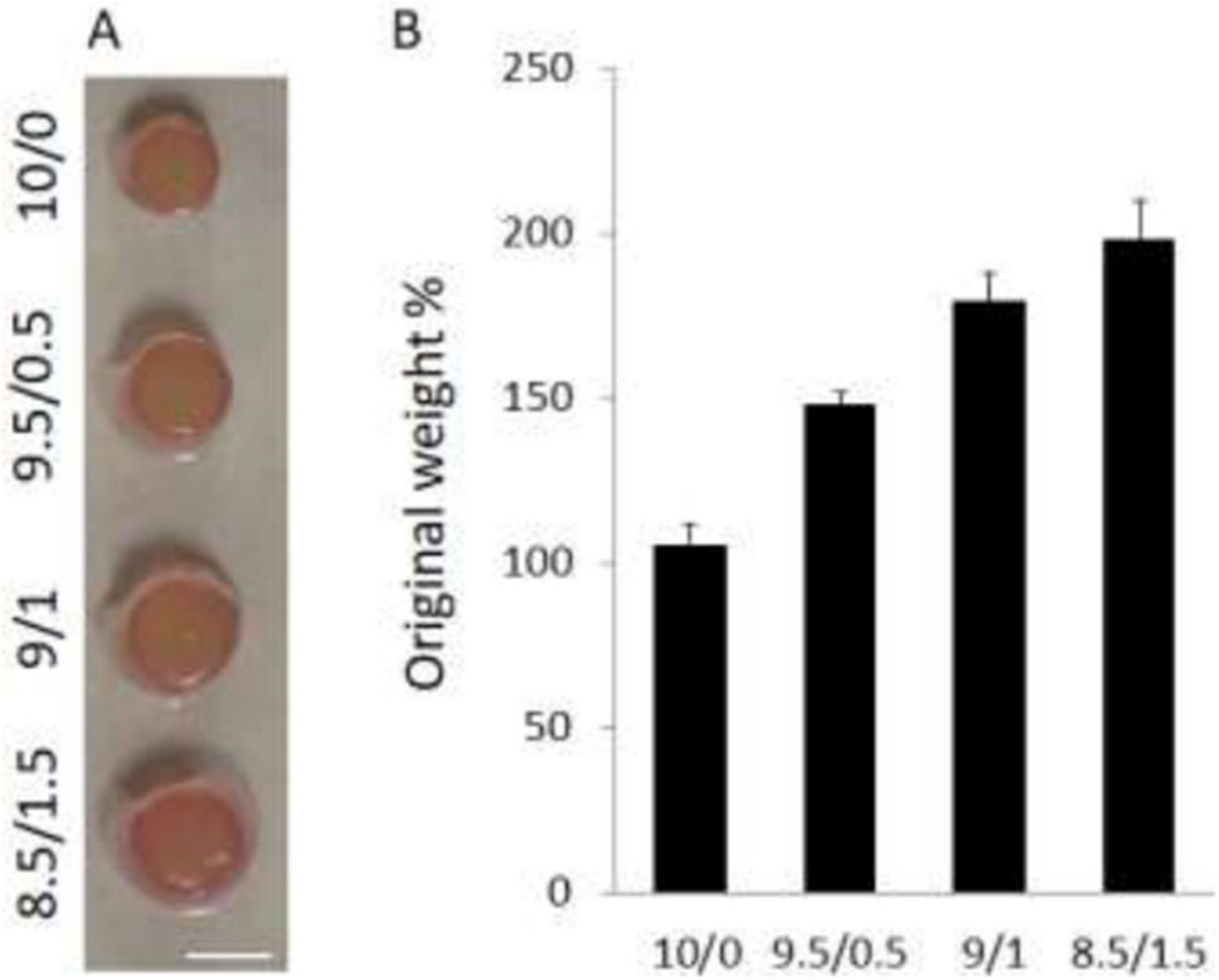

Figure 1.

After fabrication without free swelling in aqueous solution, the mechanical properties of hydrogels with different mG:mHA ratios were assessed by measuring compressive modulus. With an increase in the HA ratio, scaffolds displayed augmented mechanical properties (n=6).

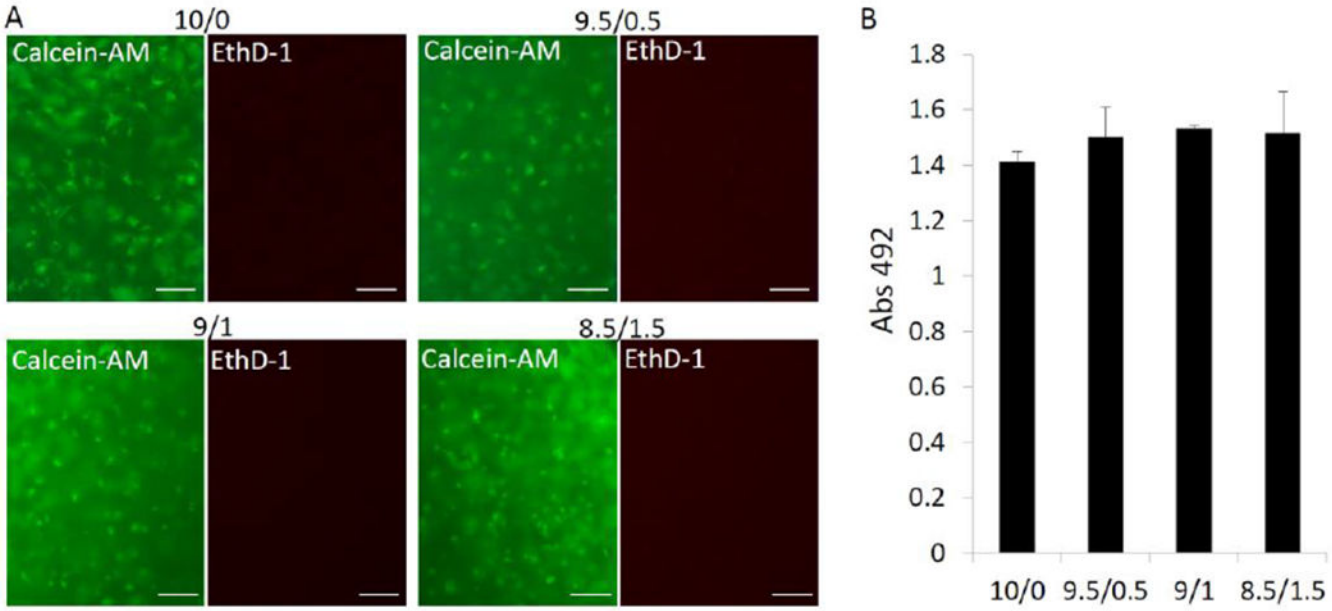

Figure 2.

Cell viability and number were estimated by live/dead staining (A) and an MTS assay, respectively. In A, live cells were stained to green using calcein-AM, and dead cells were stained to red using EthD-1. Bar=100μm; In B, no statistical difference was found (n=4).

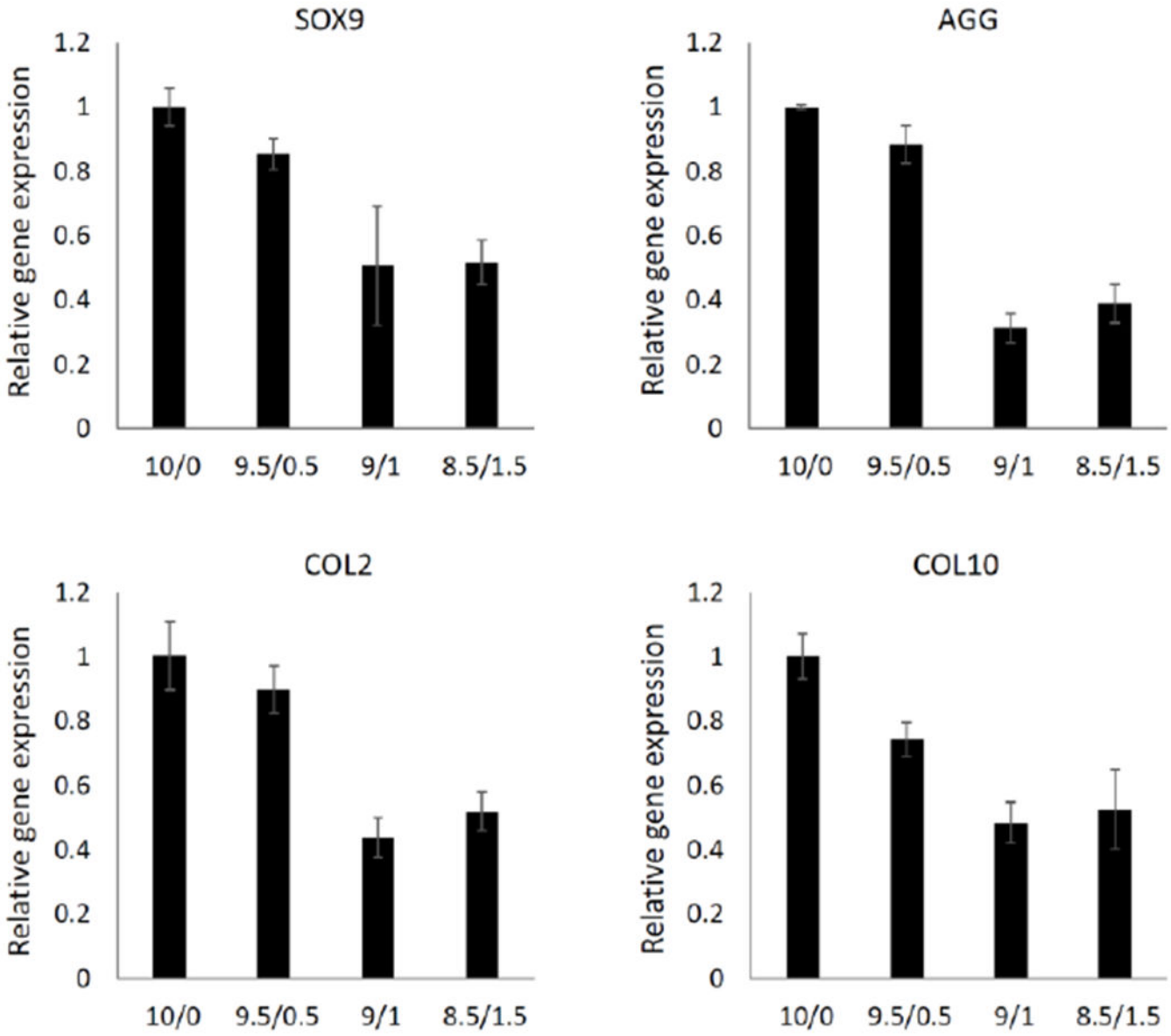

Figure 3.

Expression of chondrogenic (*SOX 9, AGG, COL2*) and hypertrophic (*COL10*) marker genes in cells within different constructs was examined after 8 weeks (n=4).

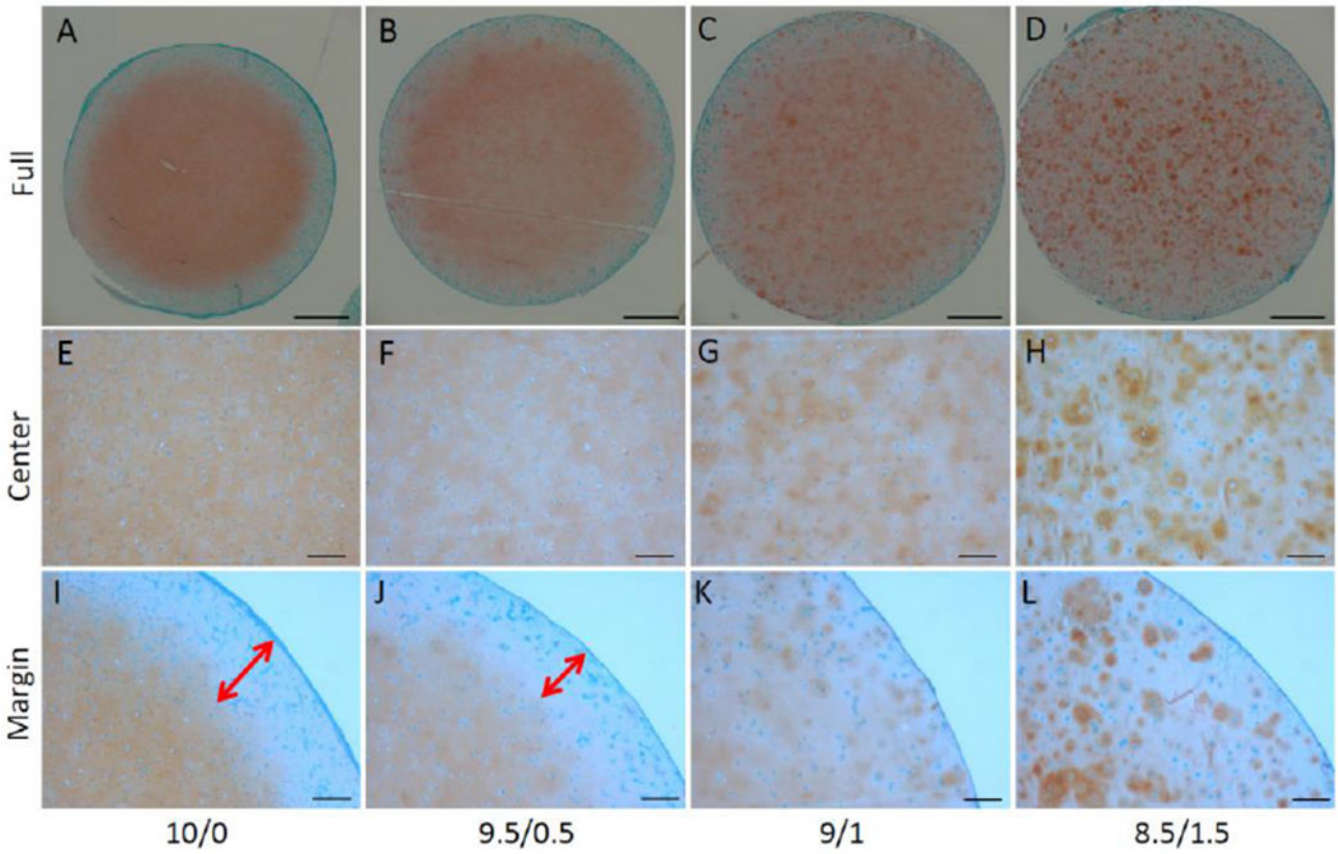

Figure 4.

Safranin O staining was used to assess the matrix content and distribution of the constructs. Two-way arrows indicated the range of GAG-free zone, which was found only in the constructs from groups 10/0 and 9.5/0.5. Bar = 1mm in A-D; 200μm in E-L.

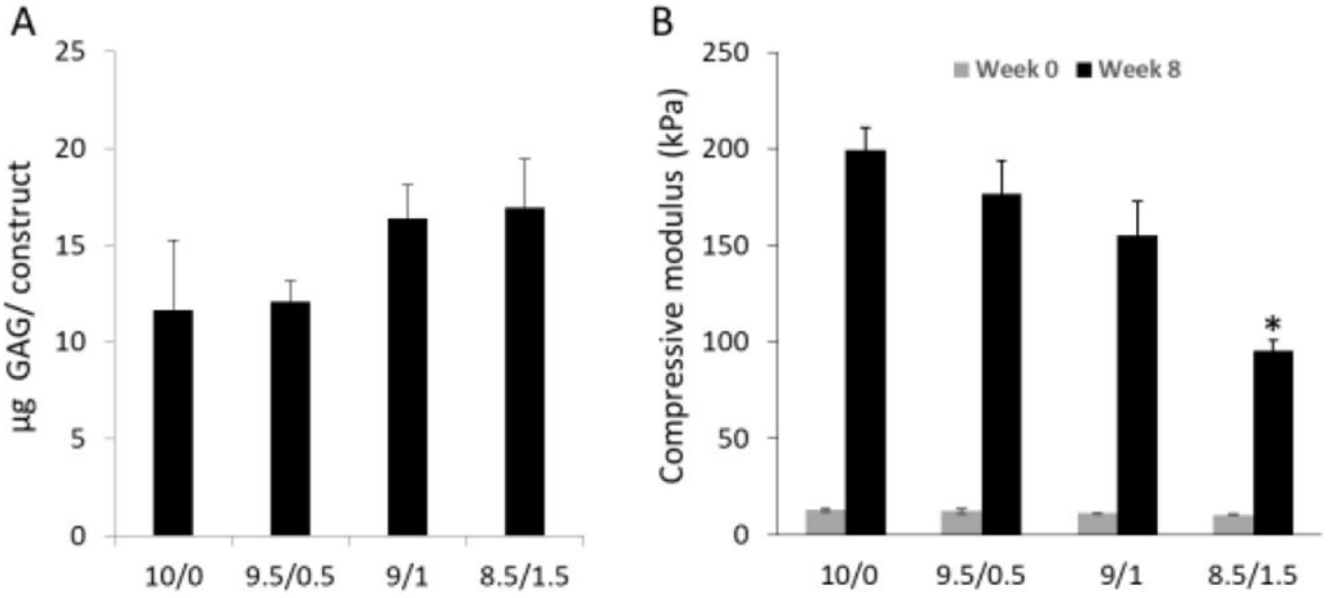

Figure 5.

GAG deposition was measured (A), and the mechanical properties of the constructs was assessed (B). (B) Compared to those at Week 0 (48 hours free swelling in medium after fabrication), constructs undergoing 8 week chondrogenesis (Week 8) displayed higher mechanical property. Interestingly, constructs in group 8.5/1/5 displayed the lowest compressive modulus, which may due to the highest swelling ratio (n=4).

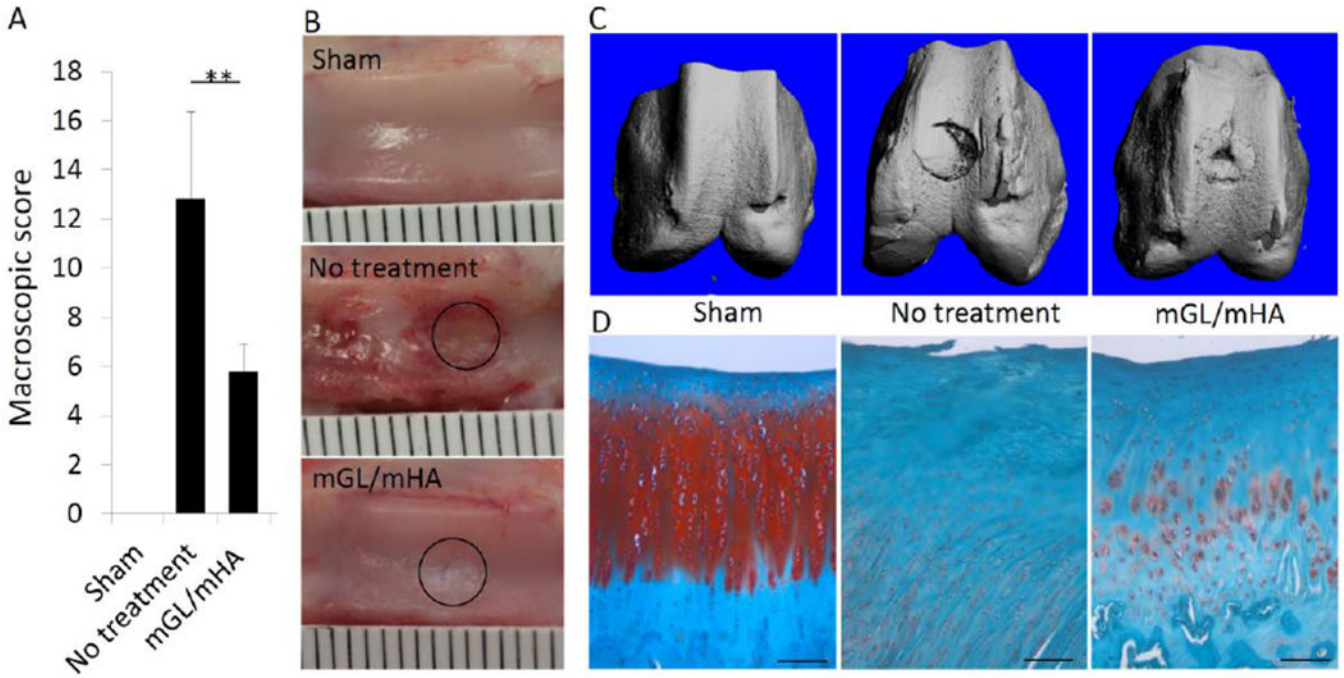

Figure 6.

Appearance of the defects (B) after 12 weeks and the score (A), with a lower score indicating better cartilage formation. μCT was used to assess subchondral bone formation (C). (D) The tissue present in the defect area was examined via histology (Safranin O staining). Sham: no osteochondral defect. No treatment: defect without treatment. mGL/mHA: defect filled with mGL/HA. Bar = 100μm in D.